Switchable Solvatochromic Probes for Live-Cell Super-resolution Imaging of Plasma Membrane Organization

Dmytro Danylchuk, Seonah Moon, Ke Xu, Andrey Klymchenko

Tailor-made switchable solvatochromic probes for live-cell super-resolution imaging of plasma membrane organization

Dmytro I. Danylchuk,[a]‡ Seonah Moon,[b], [c]‡ Ke Xu,[b], [c]* Andrey S. Klymchenko[a]*

Abstract: Visualization of the nanoscale organization of cell membranes remains challenging because of the lack of appropriate fluorescent probes. Here, we introduce a new design concept for super-resolution microscopy probes that combines specific membrane targeting, ON/OFF switching, and environment sensing functions. In this design, we propose a functionalization strategy for solvatochromic dye Nile Red that improves its photostability. The dye is grafted to a newly developed membrane-targeting moiety composed of a sulfonate group and an alkyl chain of varied lengths, which ensures high brightness and lipid-order sensitivity of the probes and tunes their binding/unbinding-induced ON/OFF switching required for single-molecule localization microscopy. While the long-chain probe with strong membrane binding, NR12A, is suitable for conventional microscopy, the short-chain probe NR4A, due to the reversible binding, enables first nanoscale cartography of the lipid order exclusively at the surface of live cells. The latter probe reveals in plasma membranes the presence of nanoscopic protrusions and invaginations of lower lipid order, suggesting a subtle connection between membrane morphology and lipid organization.

The complex nature of cell plasma membranes raised intensive research in the last decades, stimulated by the hypothesis of membrane microdomains (lipid rafts).[1] In model membranes, these domains are identified in terms of lipid order,[2] where liquid-ordered phases (Lo) rich in sphingomyelin and cholesterol “swim” in a pool of disordered phase (Ld) formed by unsaturated lipids. The challenge to visualize lipid domains in cells is linked to their highly dynamic nature, nanoscopic size, and non-flat geometry of plasma membranes with protrusions and invaginations.[3]

One approach to visualize membrane organization is fluorescent labeling of lipids, such as sphingomyelin[4] and ceramide,[5] but labeling may alter properties of lipids.[6] Another approach is to label proteins that specifically target sphingolipids,[7] although the effect of these large molecules on lipid order is still unclear. New possibilities are offered by the environment-sensitive probes,[8] sensitive to polarity (solvatochromic dyes), viscosity (molecular rotors),[9] and membrane tension (flippers).[10] The emission color of solvatochromic probes, like Laurdan,[2b] di-4-ANEPPDHQ,[11] and Nile Red,[12] directly reflects the lipid order, because it is linked with the local polarity and hydration, so that Lo and Ld phases can be distinguished in model membranes. Previously, based on Nile Red, we designed probe NR12S that reports lipid order selectively at the outer leaflet of cell plasma membranes[12]. Due to its high brightness and capacity to work at nanomolar concentrations, it became a common tool to study transmembrane asymmetry,[13] apoptosis,[14] maturation of endosomes,[15] membrane potential,[16] lipid trafficking,[17] etc.[8] The current challenge is to adapt this type of probes for super-resolution microscopy.[18]

Super-resolution microscopy, including single-molecule localization microscopy (SMLM), is making a revolution in the structural and functional characterization at the subcellular level.[3, 19] Numerous efforts have been made to develop fluorescent probes for super-resolution techniques,[20] where ON/OFF switching, required by SMLM, was implemented through photo-switching,[7a, 21] isomerization,[22] transient binding of dyes[23] and proteins[24] to the membrane, and DNA hybridization.[25] A largely underexplored direction, which can open a new dimension in SMLM, is to implement sensing function into this type of probes. It became possible with recently introduced spectrally resolved PAINT (SR-PAINT) for super-resolution imaging of biomembranes.[26] It exploits solvatochromic dye Nile Red, which (i) lights-up upon reversible binding to biomembranes[23a] and (ii) changes its emission color in response to the lipid order[6a, 8, 12, 26a, 26b]. However, this dye is not plasma membrane specific, as it binds all lipid components of cells. Here, based on Nile Red fluorophore, we designed the first probe combining together plasma membrane specificity, controlled ON/OFF switching, and sensing functions, which enabled imaging of both nanoscale morphology and lipid order in biomembranes.

To develop probes for SR-PAINT, we fundamentally changed the design strategy vs the original NR12S (Fig. 1a). First, we inverted the position of Nile Red modification and thus removed phenolic oxygen from the dye (NR12A and NR4A), which was hypothesized to cause lower photostability. Second, we propose here a new membrane-targeting moiety based on an anionic sulfonate head group and a lipophilic alkyl chain of varied lengths. We reasoned that dyes with long alkyl chains (NR12A and NR12S) should label plasma membranes quasi-irreversibly (Fig. 1b), which is suitable for conventional fluorescence microscopy. By contrast, a short alkyl chain (in NR4A) may enable reversible labeling (Fig. 1c) and thus the desired ON/OFF switching required for PAINT.[23a] Compounds NR12A and NR4A were thus synthesized in six steps starting from m-anizidine (Fig. S1).

In organic solvents of varying polarity, the absorption and emission characteristics of NR4A and NR12A were close to Nile Red (Fig. S2, Table S1), indicating that the functionalization did not perturb the fluorophore properties. All studied probes showed fluorescence intensity increase (fluorogenic response) on binding to large unilamellar vesicles (LUVs) composed of DOPC, but the titration curves varied strongly (Fig. 1d). NR12A showed significantly higher affinity to LUVs than the parent Nile Red, displaying rapid intensity growth followed by a plateau at higher concentrations, similarly to NR12S. In sharp contrast, NR4A displayed a slow increase in the fluorescence intensity with liposomes concentration, even weaker than the parent Nile Red. These results confirmed that we obtained a weak (NR4A) and a strong (NR12A) binders of lipid membranes.

[a] D. I. Danylchuk; Dr. A. S. Klymchenko
Laboratoire de Bioimagerie et Pathologies, UMR 7021 CNRS
Université de Strasbourg, 74 route du Rhin, 67401, Illkirch, France
E-mail: andrey.klymchenko@unistra.fr
[b] S. Moon; Dr. K. Xu
Department of Chemistry, University of California, Berkeley
University of California, Berkeley, California, 94720, United States
E-mail: xuk@berkeley.edu
[c] S. Moon; Dr. K. Xu
Chan Zuckerberg Biohub, San Francisco, CA 94158, United States

‡These authors contributed equally.

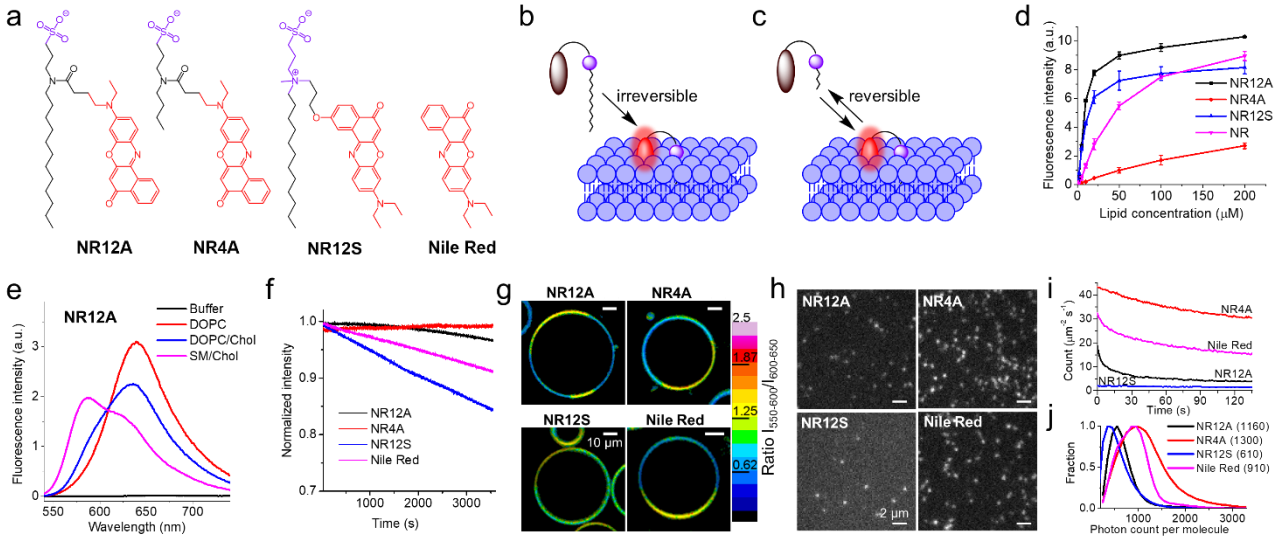

Figure 1. Design of probes and their characterization in model membranes. (a) Chemical structures of NR12A and NR4A as well as the previously reported NR12S and Nile Red. (b,c) Design concept of the fluorogenic probes that irreversibly (b) or reversibly (c) bind to biomembranes due to the presence of long or short hydrophobic chains, respectively. (d) Titration of the four membrane probes (100 nM) with increasing concentrations of lipid vesicles: fluorescence intensity at 620 nm vs. lipid concentration. Errors are s.d.m. (n = 3). (e) Fluorescence spectra of NR12A (2 μM) in buffer (20 mM phosphate buffer, pH 7.4) and liposomes (LUVs) of different lipid composition (1 mM lipids). Excitation wavelength was 520 nm. All the spectra were corrected via dividing by absorbance at the excitation wavelength. (f) Fluorescence intensity of the different probes (400 nM) under continuous illumination vs. time in DOPC liposomes (200 μM). Excitation and emission wavelengths were 540 and 620 nm, respectively. (g) Ratiometric confocal microscopy of giant vesicles composed of DOPC/SM/Chol, 1/1/0.7, stained with NR12A, NR4A, NR12S, or Nile Red (200 nM). (h) Typical single-molecule raw images recorded at 9 ms integration time (110 frames per second) in DOPC supported bilayers, for the four probes (10 nM). (i) Time-dependent counts of single molecules detected per μm^2 per second for the four probes over the full camera view. (j) Distribution of single-molecule brightness of probes in DOPC supported bilayers, expressed in terms of photon count after 50% splitting to the imaging channel. The average value for each probe is given in the legend.

Fluorescence spectra of both NR4A and NR12A (Fig. 1e, S3) exhibited blue shift by about 45-50 nm in Lo phase vesicles, composed of sphingomyelin/cholesterol (SM/Chol), compared to Ld phase vesicles, made of dioleoylphosphatidylcholine (DOPC). This behavior is similar to NR12S,[12] Nile Red (Fig. S3), and other solvatochromic probes,[2b, 11] reflecting lower local polarity/hydration in the Lo phase.[6a] Remarkably, the intensity ratio of blue to red part of emission band for both new probes was more sensitive than NR12S to lipid order (from Ld to Lo phase it increased 5.9-, 4.9- and 2.9-fold for NR4A, NR12A and NR12S, respectively), as their emission bands were narrower (Table S2). In phosphate buffer, NR12A displayed blue-shifted absorption compared to Nile Red (Table S1) and negligible fluorescence (Fig. 1e), similarly to NR12S, indicating that the NR12A forms self-quenched aggregates in water. By contrast, NR4A showed red-shifted absorption (Table S1) and non-negligible fluorescence (Fig. 1e), similarly to Nile Red, suggesting that NR4A is well dissolved and does not aggregate in water. Importantly, NR12A and NR4A displayed high fluorescence quantum yields in LUVs (39-53%, Table S1). Moreover, in DOPC LUVs they were significantly more photostable than NR12S (Fig. 1f), confirming our hypothesis on the negative effect of the phenolic oxygen on the photostability of Nile Red fluorophore. In giant unilamellar vesicles (GUVs), using two-color confocal microscopy, NR12A and NR4A provided excellent contrast between Lo phase, characterized by high intensity ratio $I_{550\text{-}600}/I_{600\text{-}650}$ (in yellow, Fig. 1g, S4), and Ld phase with low $I_{550\text{-}600}/I_{600\text{-}650}$ (in blue). The ratio changes between the two phases were higher than that of NR12S (pseudo-color change from yellow to green), in line with the spectral data in LUVs.

Single-molecule microscopy of the probes in supported DOPC lipid bilayers showed that the weak binders, NR4A and Nile Red, exhibited large number of single-molecule turn-on events that lasted well through $>10^4$ frames (Fig. 1hi, Movie S1), thanks to the continuous probe exchange between the solution and the membrane. By contrast, the strong binders, NR12A and NR12S, showed few turn-on events (Fig. 1hi), probably because most molecules were quasi-irreversibly bound to the membrane and then photobleached before single-molecule images could be recorded. Remarkably, single-molecule brightness histograms further showed that NR4A surpassed all other probes, including Nile Red, by the number of photons collected per molecule (Fig. 1j), in line with our photostability data in solution (Fig. 1f). Finally, single-molecule spectroscopy confirmed sensitivity of NR4A to lipid order in membranes (Fig. S5).

Next, the probes were incubated with HeLa cells and imaged using fluorescence microscopy (Fig. 2a). In contrast to Nile Red, showing intracellular fluorescence, NR12A exclusively stained the plasma membranes, being >2-fold brighter than NR12S. NR4A also showed specific staining for plasma membranes, but the signal was >10-fold lower, in line with its weak affinity to biomembranes. Among studied dyes only NR4A showed no signs of photobleaching (Fig. S6), which confirmed that it binds reversibly to cell membranes, so that bleached probe species are quickly replaced by intact ones, as required by PAINT.[23a] Overall, NR12A appears as a significantly improved analog of NR12S for conventional imaging, which enables, for instance, obtaining high-quality three-dimensional (3D) confocal imaging of membrane surface (Fig. 2b). Meanwhile, NR4A, for its reversible binding capability, appears promising for PAINT. NR4A is also attractive for stimulated emission depletion microscopy,[19a] because exchangeable probes solve the problem of photobleaching.[27]

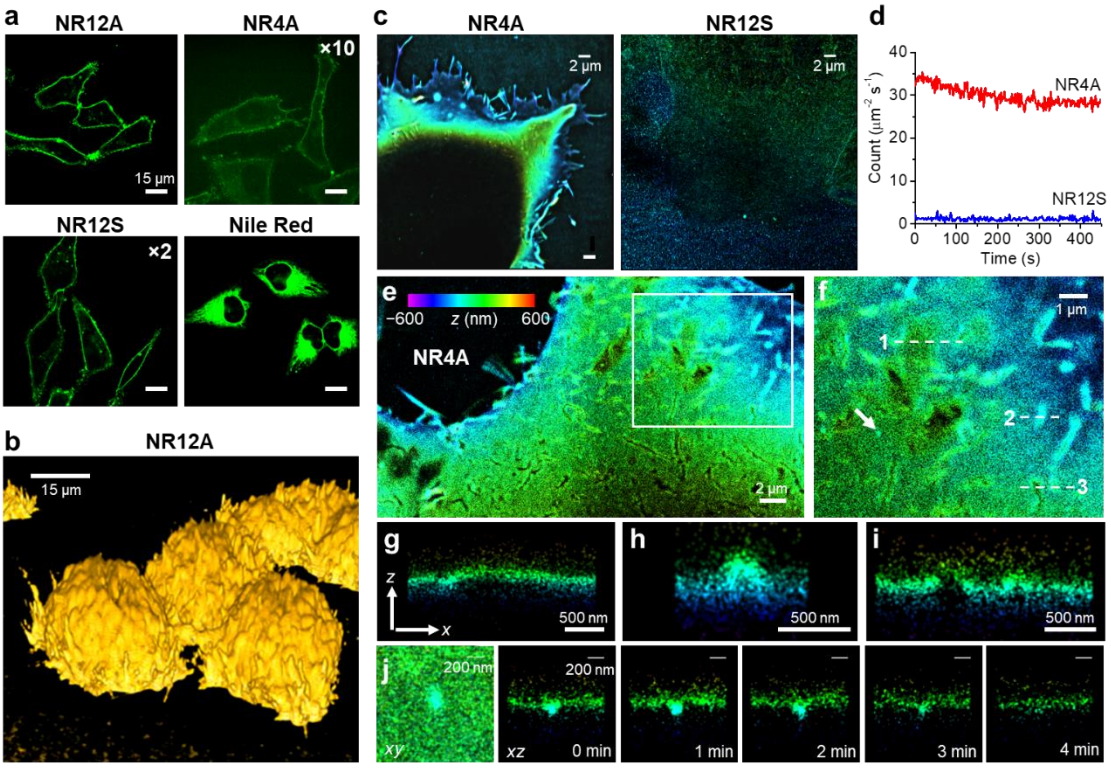

Figure 2. Cellular studies show NR12A and NR4A as superior probes for conventional and super-resolution microscopy, respectively. (a) Spinning disk confocal microscopy images of HeLa cells stained with NR12A, NR4A, NR12S, and Nile Red (20 nM) after 10 min incubation at r.t. (b) A 3D stacked image of KB cells stained with NR12A. (c) Zoom-out views of 3D PAINT results of COS-7 cells with NR4A (10 nM) and NR12S (20 nM). (d) Time-dependent counts of single molecules detected per μm^2 per second for the two probes in representative regions: 5×10^4 frames were recorded for >450 s at 110 frames per second. (e) 3D PAINT image of the top plasma membrane of a HeLa cell stained by NR4A. (f) Zoom-in of the white box in (e). (g-i) Virtual cross sections in the *xz* plane along lines 1-3 in (f). (j) Zoom-in in-plane (*xy*) image, and a time series of the vertical (*xz*) images of the endocytosis site marked by the arrow in (f). All 3D PAINT images are rendered with color to present the depth (*z*) information [color scale bar in (e)].

We then performed 3D PAINT super-resolution imaging of live cells. With 10 nM dye in the imaging medium, NR4A reversibly bound to the plasma membrane, thus achieving high counts of single molecules over 5×10^4 frames (Fig. 2d), as in supported bilayers (Fig. 1h), hence good PAINT images within 1 min acquisition (Fig. 2ce and Fig. S7). In contrast, NR12S performed poorly with low counts of single molecules (Fig. 2d), and so resulted in very dim final PAINT images (Fig. 2c). Although Nile Red also allowed decent image quality, it strongly labeled internal membranes (Fig. S8), consistent with confocal data (Fig. 2a) and previous PAINT results.[26b] We also examined CM-DiI and DiD, two common plasma membrane probes for SMLM,[28] and found both to nonspecifically label internal membranes in live cells (Fig. S8).

Owing to its high specificity, NR4A helps unveil rich nanoscale structural features of the plasma membrane (Fig. 2e-j). For HeLa cells, 3D PAINT showed numerous outward curves of the plasma membrane, including mildly bulging sites that raised up ~100 nm in height over ~1 μm lateral distances (Fig. 2fg), tube-like protrusions with higher curvatures (~100 nm radius; Fig. 2fh), as well as tall protrusions above the limit of our working z range (>400 nm above the focal plane), so that they appear dark at the center (Fig. 2fi). The observed nanoscale protrusions of the plasma membrane were highly dynamic, showing significant structural changes on the time scale of 1 minute (Fig. S8). Meanwhile, we also noted 150-200 nm-sized, pit-like invagination structures that dynamically moved into the cell on the time scale of minutes (Fig. 2j and Fig. S7), indicative of endocytosis. Similar membrane features were also observed in COS-7 cells (Fig S9).

We next exploited solvatochromism of NR4A to examine the nanoscale distribution of local chemical polarity in plasma membranes, reflecting lipid order. To this end, we performed SR-PAINT, where the fluorescence spectrum of every single molecule of NR4A was measured together with its super-localized position.[26b, 29] The obtained spectral mean, calculated as the intensity-weighted average of the emission wavelengths of each probe molecule and presented in pseudo-color, allowed us to describe local lipid order with nanometer-scale spatial resolution and minute-scale temporal resolution[26b]. In live COS-7 cells, NR4A showed a variation of pseudo-color from blue to cyan (Fig. 3ab), with the averaged single-molecule spectra peaked at ~610 nm (Fig. 3d), similar to that of Nile Red in the plasma membrane.[26b] Interestingly, upon chemical fixation, NR4A became cell permeable and so labeled internal organelle membranes with a distinct ~20 nm redshift (Fig. 3cf), similar to the results obtained earlier with Nile Red,[26b] indicating lower lipid order for the organelle membranes.

The high specificity of NR4A to the plasma membrane in live cells enabled nanoscale cartography of lipid order of cell surface, which has been a challenge so far as Nile Red exhibits strong background from internal membranes. Remarkably, for the tube-like nanoscale protrusions, in cyan pseudo-color, the locally averaged single-molecule spectra showed a ~4 nm redshift when compared to smooth parts of the plasma membrane, predominantly in blue (Fig. 3ad). This difference indicates slightly reduced local lipid order, possibly related to the dynamic structural changes of these protrusions under forces. More drastically, a strong redshift of ~20 nm, i.e., even lower lipid order, was observed for the ~200 nm-sized membrane pits (Fig. 3be), assigned above to endocytosis sites (Fig. 2j). Recent works[30] suggest that membrane curvature formation is closely related to the lipid composition. Our results above provide direct evidence

of decreased local packing orders for the highly curved structures in the plasma membrane. In view of lipid rafts hypothesis,[1] our work suggests that nanoscopic domains of low lipid order can originate from protrusions and extensions at the cell surface.

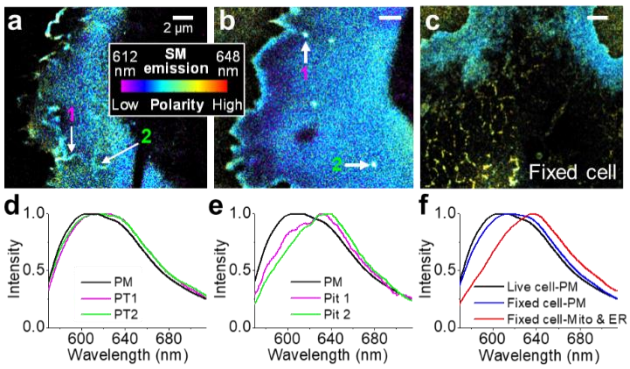

Figure 3. Nanoscopic mapping of lipid order in cell membranes with NR4A. (a,b) SR-PAINT with NR4A for the plasma membrane of live COS-7 cells. Color represents single-molecule spectral mean (color scale bar). (c) NR4A SR-PAINT for a fixed COS-7 cell, showing staining for both the plasma membrane and internal membranes. (d) Averaged single-molecule spectra at smooth parts of the plasma membrane (black) vs. at the tube-like protrusions pointed to by the two arrows in (a) (magenta and green). (e) Averaged single-molecule spectra at smooth parts of the plasma membrane (black) vs. at the cluster structures pointed to by the two arrows in (b) (magenta and green). (f) Averaged single-molecule spectra at the plasma membrane of live (black) and fixed (blue) COS-7 cells, vs. at the internal membranes of fixed COS-7 cells (red).

Thus, we introduce the concept of a fluorescent probe for super-resolution microscopy that combines target specificity, ON/OFF switching, and polarity sensing. It was realized based on solvatochromic dye Nile Red and a newly introduced low-affinity membrane binder that ensures reversible bind/unbinding events and targets specifically cell plasma membranes. The developed probe (NR4A) revealed lipid order heterogeneity at the cell surface and its connection to nanoscale membrane topology.

Acknowledgements

This work was supported by the European Research Council ERC Consolidator grant BrightSens 648528 and the National Science Foundation (CHE-1554717). K.X. is a Chan Zuckerberg Biohub investigator. S.M. acknowledges support from a Samsung Scholarship. Bohdan Wasylyk is acknowledged for providing the KB cells.

Keywords: Fluorescent probes • solvatochromism • membranes • super-resolution microscopy • lipid order

[1] a) D. Lingwood, K. Simons, *Science* **2010**, *327*, 46; b) E. Sezgin, I. Levental, S. Mayor, C. Eggeling, *Nat. Rev. Mol. Cell Biol.* **2017**, *18*, 361.

[2] a) T. Baumgart, S. T. Hess, W. W. Webb, *Nature* **2003**, *425*, 821; b) C. Dietrich, L. A. Bagatolli, Z. N. Volovyk, N. L. Thompson, M. Levi, K. Jacobson, E. Gratton, *Biophys. J.* **2001**, *80*, 1417.

[3] M. B. Stone, S. A. Shelby, S. L. Veatch, *Chem. Rev.* **2017**, *117*, 7457.

[4] M. Kinoshita, K. G. Suzuki, N. Matsumori, M. Takada, H. Ano, K. Morigaki, M. Abe, A. Makino, T. Kobayashi, K. M. Hirosawa, T. K. Fujiwara, A. Kusumi, M. Murata, *J. Cell. Biol.* **2017**, *216*, 1183.

[5] A. Burgert, J. Schlegel, J. Becam, S. Doose, E. Bieberich, A. Schubert-Unkmeir, M. Sauer, *Angew. Chem. Int. Ed. Engl.* **2017**, *56*, 6131.

[6] a) A. S. Klymchenko, R. Kreder, *Chem. Biol.* **2014**, *21*, 97; b) E. Sezgin, I. Levental, M. Grzybek, G. Schwarzmann, V. Mueller, A. Honigmann, V. N. Belov, C. Eggeling, U. Coskun, K. Simons, P. Schwille, *Biochim. Biophys. Acta-Biomembr.* **2012**, *1818*, 1777.

[7] a) H. Mizuno, M. Abe, P. Dedecker, A. Makino, S. Rocha, Y. Ohno-Iwashita, J. Hofkens, T. Kobayashi, A. Miyawaki, *Chemical Science* **2011**, *2*, 1548; b) F. Hullin-Matsuda, M. Murate, T. Kobayashi, *Chem. Phys. Lipids* **2018**, *216*, 132.

[8] A. S. Klymchenko, *Acc. Chem. Res.* **2017**, *50*, 366.

[9] J. E. Chambers, M. Kubankova, R. G. Huber, I. Lopez-Duarte, E. Avezov, P. J. Bond, S. J. Marciniak, M. K. Kuimova, *ACS Nano* **2018**, *12*, 4398.

[10] A. Colom, E. Derivery, S. Soleimanpour, C. Tomba, M. Dal Molin, N. Sakai, M. Gonzalez-Gaitan, S. Matile, A. Roux, *Nat. Chem.* **2018**, *10*, 1118.

[11] L. Jin, A. C. Millard, J. P. Wuskell, X. M. Dong, D. Q. Wu, H. A. Clark, L. M. Loew, *Biophys. J.* **2006**, *90*, 2563.

[12] O. A. Kucherak, S. Oncul, Z. Darwich, D. A. Yushchenko, Y. Arntz, P. Didier, Y. Mely, A. S. Klymchenko, *J. Am. Chem. Soc.* **2010**, *132*, 4907.

[13] S. Chiantia, P. Schwille, A. S. Klymchenko, E. London, *Biophys J* **2011**, *100*, L1.

[14] R. Kreder, K. A. Pyrshev, Z. Darwich, O. A. Kucherak, Y. Mely, A. S. Klymchenko, *ACS chemical biology* **2015**, *10*, 1435.

[15] Z. Darwich, A. S. Klymchenko, D. Dujardin, Y. Mely, *Rsc Advances* **2014**, *4*, 8481.

[16] M. Sundukova, E. Prifti, A. Bucci, K. Kirillova, J. Serrao, L. Reymond, M. Umebayashi, R. Hovius, H. Riezman, K. Johnsson, P. A. Heppenstall, *Angew. Chem. Int. Ed.* **2019**, *58*, 2341.

[17] a) J. Kim, A. Singh, M. Del Poeta, D. A. Brown, E. London, *J. Cell Sci.* **2017**, *130*, 2682; b) D. B. Iaea, F. R. Maxfield, *PloS one* **2017**, *12*, e0188041.

[18] E. Sezgin, F. Schneider, V. Zilles, I. Urbancic, E. Garcia, D. Waithe, A. S. Klymchenko, C. Eggeling, *Biophys. J.* **2017**, *113*, 1321.

[19] a) S. J. Sahl, S. W. Hell, S. Jakobs, *Nat. Rev. Mol. Cell Biol.* **2017**, *18*, 685; b) Y. M. Sigal, R. Zhou, X. Zhuang, *Science* **2018**, *361*, 880.

[20] a) J. B. Grimm, B. P. English, J. J. Chen, J. P. Slaughter, Z. J. Zhang, A. Revyakin, R. Patel, J. J. Macklin, D. Normanno, R. H. Singer, T. Lionnet, L. D. Lavis, *Nat. Methods* **2015**, *12*, 244; b) H. L. Li, J. C. Vaughan, *Chem. Rev.* **2018**, *118*, 9412; c) L. Wang, M. S. Frei, A. Salim, K. Johnsson, *J. Am. Chem. Soc.* **2018**, *141*, 2770; d) G. T. Dempsey, J. C. Vaughan, K. H. Chen, M. Bates, X. W. Zhuang, *Nat. Methods* **2011**, *8*, 1027.

[21] a) M. J. Rust, M. Bates, X. W. Zhuang, *Nat. Methods* **2006**, *3*, 793; b) S. Habuchi, R. Ando, P. Dedecker, W. Verheijen, H. Mizuno, A. Miyawaki, J. Hofkens, *Proc. Natl. Acad. Sci. U. S. A.* **2005**, *102*, 9511.

[22] S. N. Uno, M. Kamiya, T. Yoshihara, K. Sugawara, K. Okabe, M. C. Tarhan, H. Fujita, T. Funatsu, Y. Okada, S. Tobita, Y. Urano, *Nature Chemistry* **2014**, *6*, 681.

[23] a) A. Sharonov, R. M. Hochstrasser, *Proc. Natl. Acad. Sci. U. S. A.* **2006**, *103*, 18911; b) C. K. Spahn, M. Glaesmann, J. B. Grimm, A. X. Ayala, L. D. Lavis, M. Heilemann, *Sci. Rep.* **2018**, *8*, 14768.

[24] S. Rocha, J. A. Hutchison, K. Peneva, A. Herrmann, K. Müllen, M. Skjøt, C. I. Jørgensen, A. Svendsen, F. C. De Schryver, J. Hofkens, H. Uji-i, *ChemPhysChem* **2009**, *10*, 151.

[25] R. Jungmann, M. S. Avendano, M. J. Dai, J. B. Woehrstein, S. S. Agasti, Z. Feiger, A. Rodal, P. Yin, *Nat. Methods* **2016**, *13*, 439.

[26] a) M. N. Bongiovanni, J. Godet, M. H. Horrocks, L. Tosatto, A. R. Carr, D. C. Wirthensohn, R. T. Ranasinghe, J. E. Lee, A. Ponjavic, J. V. Fritz, C. M. Dobson, D. Klenerman, S. F. Lee, *Nat. Commun.* **2016**, *7*, 13544; b) S. Moon, R. Yan, S. J. Kenny, Y. Shyu, L. M. Xiang, W. Li, K. Xu, *J. Am. Chem. Soc.* **2017**, *139*, 10944; c) R. Yan, S. Moon, S. J. Kenny, K. Xu, *Acc. Chem. Res.* **2018**, *51*, 697.

[27] C. Spahn, J. B. Grimm, L. D. Lavis, M. Lampe, M. Heilemann, *Nano Letters* **2019**, *19*, 500.

[28] S. H. Shim, C. Xia, G. Zhong, H. P. Babcock, J. C. Vaughan, B. Huang, X. Wang, C. Xu, G. Bi, X. Zhuang, *Proc. Natl. Acad. Sci. U. S. A.* **2012**, *109*, 13978.

[29] Z. Zhang, S. J. Kenny, M. Hauser, W. Li, K. Xu, *Nature Methods* **2015**, *12*, 935.

[30] a) S. Vanni, H. Hirose, H. Barelli, B. Antonny, R. Gautier, *Nature communications* **2014**, *5*, 4916; b) M. Pinot, S. Vanni, S. Pagnotta, S. Lacas-Gervais, L.-A. Payet, T. Ferreira, R. Gautier, B. Goud, B. Antonny, H. Barelli, *Science* **2014**, *345*, 693.

Entry for the Table of Contents

COMMUNICATION

Targeting, switching and sensing were combined together in one fluorescent probe to achieve nanoscale cartography of cell plasma membranes. The proposed design is based on a new functionalization strategy of solvatochromic dye Nile Red, sensitive to lipid order, and a special membrane-targeting moiety that controls binding/unbinding-induced ON/OFF switching for super-resolution microscopy.

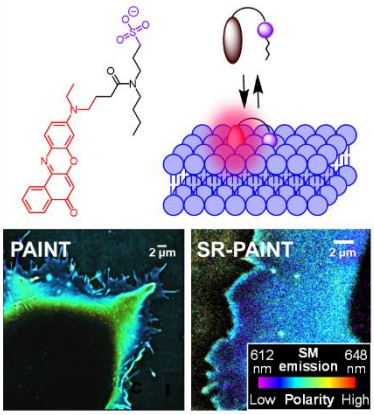

Dmytro I. Danylchuk, Seonah Moon, Ke Xu, Andrey S. Klymchenko**

Page No. – Page No.

Tailor-made switchable solvatochromic probes for live-cell super-resolution imaging of plasma membrane organization